


An Increase of Excitatory-to-Inhibitory Synaptic Balance in the Contralateral Cortico-Striatal Pathway Underlies Improved Stroke Recovery in BDNF Val66Met SNP Mice

Neurorehabilitation and Neural Repair
 2019, Vol. 33(12) 989–1002
 © The Author(s) 2019
 Article reuse guidelines:
sagepub.com/journals-permissions
 DOI: 10.1177/1545968319872997
journals.sagepub.com/home/nnr


Luye Qin, PhD^{1,2}, Hannah S. Actor-Engel³ , Moon-Sook Woo, PhD¹, Faariah Shakil¹, Yi-Wen Chen, PhD³, Sunghoo Cho, PhD^{1,4}, and Chiye Aoki, PhD^{3,5}

Abstract

Despite negative association in cognition and memory, mice harboring *Val66Met* BDNF SNP (BDNF^{M/M}) exhibit enhanced motor recovery accompanied by elevated excitatory synaptic markers VGLUT1 and VGLUT2 in striatum contralateral to unilateral ischemic stroke. The cortico-striatal pathway is a critical gateway for plasticity of motor/gait function. We hypothesized that enhanced excitability of the cortico-striatal pathway, especially of the contralateral hemisphere, underlies improved motor recovery. To test this hypothesis, we examined the key molecules involving excitatory synaptogenesis: Thrombospondins (TSP1/2) and their neuronal receptor $\alpha 2\delta$ -1. In WT brains, stroke induced expressions of TSP1/2-mRNA. The contralateral hemisphere of BDNF^{M/M} mice showed heightened TSP2 and $\alpha 2\delta$ -1 mRNA and protein specifically at 6 months post-stroke. Immunoreactivities of TSPs and $\alpha 2\delta$ -1 were increased in cortical layers 1/2 of stroked BDNF^{M/M} animals compared with BDNF^{M/M} sham brains at this time. Areal densities of excitatory synapses in cortical layer I and striatum were also increased in stroked BDNF^{M/M} brains, relative to stroked WT brains. Notably, the frequency of GABAergic synapses was greatly reduced along distal dendrites in cortical layer I in BDNF^{M/M} brains, whether or not stroked, compared with WT brains. There was no effect of genotype or treatment on the density of GABAergic synapses onto striatal medium spiny neurons. The study identified molecular and synaptic substrates in the contralateral hemisphere of BDNF^{M/M} mice, especially in cortical layers 1/2, which indicates selective region-related synaptic plasticity. The study suggests that an increase in excitatory-to-inhibitory synaptic balance along the contralateral cortico-striatal pathway underlies the enhanced functional recovery of BDNF^{M/M} mice.

Keywords

BDNF, SNP, neural circuit, cortico-striatal pathway, stroke, recovery

Introduction

Genetic variants contribute to injury-induced structural plasticity and behavioral adaptation. However, the underlying mechanisms by which genetic variants affect recovery in stroke are not well understood. Brain-derived neurotrophic factor (BDNF) is a widely expressed neurotrophin in the central nervous system (CNS) and plays an important role in synaptic plasticity, memory, and cognition.^{1,2} A variant of the BDNF gene with a single nucleotide polymorphism (SNP) at codon 66 has been identified in humans. The presence of this SNP is negatively associated with cognition and memory and reduces activity-dependent BDNF secretion.³ The effects of *Val66Met* SNP on stroke outcome and rehabilitation remains to be fully elucidated.⁴ Earlier studies in stroke patients indicate a primarily maladaptive role with *Met* carriers, based on worse functional outcomes.^{5,6} Other

studies indicated that *Val66Met* SNP is associated with worse outcomes at early but not at later time points.^{7,8} Moreover, under certain conditions, it can promote improved outcomes.⁹

¹Burke Neurological Institute, White Plains, NY, USA

²State University of New York at Buffalo, Buffalo, NY, USA

³New York University, New York, NY, USA

⁴Weill Cornell Medical College, New York, NY, USA

⁵NYU Langone Medical Center, New York, NY, USA

Corresponding Authors:

Sunghoo Cho, Feil Family Brain and Mind Research Institute, Weill Cornell Medical College Burke Neurological Institute, 785 Mamaroneck Avenue, White Plains, NY 10605, USA.
 Email: suc2002@med.cornell.edu

Chiye Aoki, Center for Neural Science, New York University, 4 Washington Place, New York, NY 10003, USA.
 Email: ca3@nyu.edu

Mice harboring the human BDNF Val66Met at both alleles (BDNF^{M/M}) display an anxiety phenotype and memory deficit, recapitulating traits in humans who carry the SNP. Previously, we reported that BDNF^{M/M} mice exhibit greater acute motor deficits but unexpected enhancement of motor/gait function during the subacute and long-term recovery phase following stroke.¹⁰ The enhanced functional recovery in BDNF^{M/M} was pronounced in the ipsilesional limbs, suggesting the involvement of contralateral hemisphere. The elevated expressions of excitatory synaptic markers VGLUT1/2 in the contralateral striatum suggested a link between excitatory synaptic substrates and superior stroke recovery.

Thrombospondins (TSPs) are large oligomeric extracellular glycoproteins that engage in cell-matrix interactions and are implicated in multiple pathophysiological states.¹¹ They play a major role in tissue remodeling and regulate synaptogenesis in the CNS.^{12,13} Secreted by astrocytes, TSP1/2 are considered to be essential signals for excitatory synapse formation.^{13,14} The formation of excitatory synapses is mediated through the binding of TSPs to the $\alpha 2\delta$ -1, an auxiliary subunit of calcium channel. $\alpha 2\delta$ -1 was identified as the neuronal TSP receptors responsible for the formation of CNS excitatory synapses.¹⁵ Overexpression of $\alpha 2\delta$ -1 increases excitatory connections, while the loss of $\alpha 2\delta$ -1 profoundly reduces the number of excitatory synapses.^{16,17} This indicates the role of TSPs/ $\alpha 2\delta$ -1 interactions in excitatory synaptogenesis.

Functional recovery from stroke and repair of other CNS injuries requires enhanced synaptic plasticity.^{18,19} A shift in synaptic balance toward excitation, either by elevating excitatory markers or reducing inhibitory signals, has been implicated in the improvement of stroke recovery.^{10,20} Given the fact that TSPs expressions increase in post-stroke brains,^{21,22} and that the TSPs/ $\alpha 2\delta$ -1 interaction contributes to excitatory synaptic formation, we sought to determine whether TSPs/ $\alpha 2\delta$ -1 are the molecular and synaptic substrates that account for the superior recovery in BDNF^{M/M} mice. We hypothesized that improved motor recovery of BDNF^{M/M} mice is due to increases in the expressions of TSPs and $\alpha 2\delta$ -1 at excitatory synapses in the contralateral hemispheres, which enhances excitatory-to-inhibitory balance at synapses of the cortico-striatal pathway in the post-stroke brain. Here we show that, indeed, stroke increases excitatory synaptic markers and synapses and reduces inhibitory synapses in the contralateral cortico-striatal pathway of BDNF^{M/M} mice. Moreover, we demonstrate that layers 1/2 of contralateral cortex is a site of synaptic plasticity.

Methods

Animals

Procedures for the use of animals were approved by the Institutional Animal Care and Use Committee (IACUC) of

Weill Cornell Medicine, National Institutes of Health, and ARRIVE (Animal Research: Reporting of In Vivo Experiments) guidelines. C57bl/6, BDNF^{+/+} (wild type, WT) and BDNF^{M/M} male mice (3–4 months) were used. We used BDNF^{+/+} and BDNF^{M/M} littermates from respective 12x heterozygote mating to match the genetic background within a given experiment for the controlled preclinical studies described.³ The facility monitors and maintains temperature, humidity, and a 12-hour light/dark cycle. Because of the nature of a long-term study, mice were given a code (either tattoo or ear tag) at the beginning of the study. Surgeons who performed sham or transient middle cerebral artery occlusion (MCAO) were blinded to the animals. Animals' identity was also blinded to the persons who cryo-sectioned, vibratome-sectioned, or ultrathin-sectioned and evaluated outcomes. Sample size for stroke outcome measurements was calculated a priori to be a minimum 10 by predicting detectable differences to reach a power of 0.80 at a significance level of <.05, assuming a 40% difference in mean and a 30% standard deviation²³ at the 95% confidence level.

MCAO and Chronic Recovery Model

Male WT and BDNF^{M/M} mice at 3 to 4 months of age were randomly assigned to undergo sham or MCAO by using 6-0 Teflon-coated monofilament surgical sutures (Doccol Co) for 30 minutes as previously described.^{24,25} Sham surgery consisted of exposure of the right carotid artery at its bifurcation without occlusion under the same duration of anesthesia. The transient MCAO perturbed blood flow in the striatum, thalamus, and the cortex unilaterally with the striatum as the structure most affected by the occlusion. Body temperature was maintained at 37°C \pm 0.5°C before, during, reperfusion phases as well as 45 minutes of post-stroke recovery period. A sizable infarction of around 35 mm³ (~20% ipsilesional hemisphere) in the MCA territory was produced at 3 days post-stroke,²⁴ which was accompanied by acute motor and gait impairment, but with substantial spontaneous recovery by 2 weeks. Prior to returning to home cages, mice were placed in a recovery cage while maintaining body temperature 37°C \pm 0.5°C until the animal regained consciousness and resumed activity. Animals that exhibited both cerebral blood flow (CBF) reduction of more than 80% during MCAO and CBF recovery of more than 80% by 10 minutes after reperfusion were included in the study. Saline was subcutaneously administered daily and Hydrogel (ClearH²O) was given to prevent dehydration during the first week of the post-stroke period twice a day. Mice typically started to regain body weight around days 5 to 6 and continued to recover from stroke.

Tissue Preparation for Molecular Analyses

As reported in a previous study,²⁶ sections were collected for each hemisphere to perform molecular analyses at

indicated time points from the brain regions spanning about 7 mm rostrocaudal (+2.8 to -3.8mm from bregma covering entire infarct region), including both cortex and striatum.

TSP1/2, α 2 δ -1, and PSD-95 mRNA

Measurement

mRNA levels were quantified with real-time reverse transcription-polymerase chain reaction (RT-PCR) using fluorescent TaqMan technology as described previously.^{27,28} PCR primers and probes specific for the genes in this study were obtained as TaqMan predeveloped assay reagents for gene expression (Life Technologies, Foster City, CA). Primers used were TSP1 (Mm01335418_m1), TSP2 (Mm01279240_m1), α 2 δ -1 (Mm00486607_m1), PSD-95 (Mm00492193_m1), and β -actin (Mm00607939_s1). β -Actin was used as an internal control for normalization of samples. The PCR was performed in 20 μ L total volume using FastStart Universal Probe Master Mix (Roche, Indianapolis, IN) by incubating at 95°C for 10 minutes followed by 40 cycles of 15 seconds at 95°C and 1 minute at 60°C. The results were analyzed using 7500 Fast Real-Time PCR System software (Life Technologies, Grand Island, NY).

α 2 δ -1 Protein Measurement

Brain sections were homogenized in CelLytic buffer (Sigma, MO) containing protease inhibitors (Roche). Fifty micrograms of protein were loaded on a NuPAGE 4% to 12% Bis-Tris Gel (Life Technologies) and transferred onto a polyvinylidene fluoride membrane (Bio-Rad, Hercules, CA). Briefly, the membrane was incubated at 4°C with α 2 δ -1 (D219, 1:1,000 Sigma) or β -actin (sc-1615, 1:10,000, Santa Cruz Biotechnology) antibody overnight. Membranes were incubated with secondary antibodies conjugated with Alexa Fluor 680 (A 21088, Life Technologies), or IRDye 680RD (926-68071, Li-cor). Each protein's specific band was visualized using the Odyssey Imaging System (Li-cor).

Tissue Preparation for Light and Electron Microscopy (LM and EM)

Three- to 4-month-old BDNF^{+/+} and BDNF^{M/M} mice underwent either sham or MCAO. Six months after, animals were anesthetized and transcardially perfused with a fixative consisting of 4% paraformaldehyde buffered by 0.1 M phosphate buffer. Brains were postfixed for a minimum of 3 days before preparing coronal sections using a vibrating microtome set at a thickness of 50 μ m. Sections were allocated across three staining procedures: LM-immunocytochemistry (LM-ICC) to measure regional densities of α 2 δ -1; EM-ICC to detect areal frequencies of inhibitory synapses formed by axon terminals immunoreactive for the GABAergic marker, glutamic

acid decarboxylase (GAD); and EM without ICC to quantify the areal density of excitatory axo-spinous synapses formed onto pyramidal neurons in cortex and medium spiny neurons (MSN) in striatum, so identified based on the morphology of the synapses as asymmetric and with thick postsynaptic densities (PSDs), formed on dendritic spine heads.

LM-ICC Detection of TSP1/2, α 2 δ -1

One section containing the cortico-striatal path was chosen randomly from a collection of 50 μ m vibratome sections of each animal. Briefly, free-floating sections were incubated with mouse anti-thrombospondins (1:100, Abcam ab1823), or mouse anti- α 2 δ -1 (1:100, Sigma D219) and secondary antibody (1:2000, Alexa Fluor 594). The negative control sample was treated with the absence of primary antibody. Images were obtained all at once using an inverted Nikon Eclipse Ti-U confocal microscope.

LM-ICC Detection of α 2 δ -1 With Silver-Intensified Gold (SIG) and Quantification

Specificity of the α 2 δ -1 antibody (Sigma D219) was previously validated.²⁹ One section containing the cortico-striatal path was packed randomly from a collection of vibratome sections of each animals. Briefly, free-floating sections were incubated with mouse anti- α 2 δ -1 (1:100, Sigma D219). Immunoreactivity was detected by the SIG procedure using goat anti-mouse IgG conjugated to 0.8-nm colloidal gold (1:100, EMSciences Cat No. 25121), as described previously.³⁰ All sections were scanned at once, using VS120 (Olympus) at a magnification of 2 \times and 10 \times . Auto-corrections were turned off to avoid introducing interanimal variabilities arising from the image capturing step. The gray values ranged from 0 to 255, with higher values indicating less labeling. The background gray values were measured from tissue that underwent the identical ICC procedure³⁰ in parallel but for which the initial incubation was performed in the absence of primary antibody. The difference in the measured greyscale values from the background values was plotted using reversed gray scale, whereby the background was equal to zero.

EM Detection of Axospinous Synapses and Quantification

Two brain subregions were analyzed: Layer 1 of cerebral cortex for the analysis of excitatory axo-spinous synapses onto apical dendritic tuft spines of pyramidal neurons, and dorsolateral striatum for the analysis of excitatory axo-spinous synapses onto MSN. The sample size per brain region per animal was equalized across animals. Excitatory axo-spinous synapses were identified using criteria used previously³¹ by the presence of thick PSDs within spines that

were devoid of mitochondria, gathering of small clear vesicles in axon terminals, and parallel alignment of the plasma membrane of the axon terminal facing the spine plasma membrane associated with the PSD. The electron microscopists capturing images were kept blind about the treatment and genotype of animals from which the tissue was derived.

EM-ICC Detection of GAD and Quantification of GABAergic Synapses

Specificity of the antibody used to detect GAD65 and GAD67 isoforms (AB1511, Chemicon,) was established previously.^{32,33} The procedure for EM-ICC and quantification of GABAergic synapses was performed as described previously using HRP-DAB (horseradish peroxidase–3,3'-diaminobenzidine) as the immunolabel.³³ EM samples were imaged strictly in the order of encounter from portions of the ultrathin sections showing the tissue-to-plastic transition, so as to ensure random sampling from a portion of the vibratome section that was nearest to the surface where access to immunoreagents would be the greatest. The sample size per brain region per animal was equalized. For the assessment of the proportion of layer 5 pyramidal cell body plasma membrane contacted GABAergic axosomatic synapse lengths, 5 cell bodies per brain region per animal were analyzed. To assess the proportion of the plasma membrane of spiny dendrites in layer 1 and dorsal striatum that were contacted by GABAergic axon terminals, 10 dendritic profiles were sampled from each brain, using electron micrographs that were captured at a magnification of 25000 \times . All quantifications were performed while kept blind of the treatment and genotype.

Statistical Analyses

mRNA levels were expressed as mean \pm standard error of the mean (mean \pm SEM) and statistical comparison were made using 1-way analysis of variance followed by post hoc tests for multiple comparison and the Student's *t* test for 2 groups. For LM and EM studies, the Kruskal-Wallis non-parametric test was used, followed by uncorrected Dunn's test for multiple comparisons to identify genotype and treatment effects. Differences were considered statistically significant at $P < .05$.

Results

TSP2 Expression in Brain Is Elevated in BDNF^{M/M} Mice at 6 Months After Stroke

Stroke increases the expressions of TSPs in acute and subacute phases of stroke.²¹ To address changes of TSP genes during stroke recovery, their expressions were measured in the brains of WT mice between 2 weeks to 6 months post-stroke. The hemisphere contralateral to unilateral ischemic stroke showed

a moderate but significant elevation of TSP1-, but not TSP2-mRNA levels, compared with pre-stroke levels (Figure 1A and B). There were significant upregulations of TSP1 and 2 in the stroke hemisphere at 2 weeks and 2 months after stroke. The chronic upregulation of TSPs in both hemispheres suggests a contributing role of TSPs to continual tissue remodeling in both hemispheres following stroke.

Prompted by a previous finding of increased striatal volume and in the contralateral hemisphere in BDNF^{M/M} mice at 6 months post-stroke,¹⁰ we sought to determine the effect of a BDNF SNP on stroke-induced TSPs expressions. Compared with WT mice, there was no noticeable increase in TSP1 mRNA levels in the BDNF^{M/M} mice after stroke, where TSP1 mRNA shows a significant reduction in the ipsilateral hemisphere (Figure 1C). However, TSP2 gene expression was significantly increased in both hemispheres of BDNF^{M/M} mice at 6 months after stroke, but not at earlier time points (Figure 1D). The upregulation of TSP2 gene expression was more pronounced in the contralateral hemispheres. The immunoreactivity of TSP1/2 revealed a widespread expression in cerebral cortex with stronger immunoreactivity in layer 2 of cerebral cortex (Figure 1E), and much less immunoreactivity in striatum (inset). Mean optical intensities of TSP in cortical layers 1 and 2 show a trend of increase in BDNF^{M/M} stroke animals compared to BDNF^{+/+} stroke mice (Figure 1F). However, TSP immunoreactivity in layer 2 in BDNF^{M/M} stroke mice showed significantly higher intensity than BDNF^{+/+}-stroke mice when immunoreactivity in layer 4 was subtracted as the internal background ($P < .05$).

Increased $\alpha 2\delta$ -1 Expression in the Contralateral Hemisphere of BDNF^{M/M} Mice 6 Months After Stroke

The gene expression profiles of $\alpha 2\delta$ -1, a neuronal receptor for TSPs, and PSD-95, an excitatory postsynaptic marker, were determined. Unlike TSPs, stroke-induced attenuation in the genes' expressions of $\alpha 2\delta$ -1 and PSD-95 throughout the recovery phase spanning from 2 weeks to 6 months after stroke (Figure 2A and B). We found no significant differences in the expressions of $\alpha 2\delta$ -1 and PSD-95 in BDNF^{+/+} and BDNF^{M/M} brains at early time points (2 weeks and 1 month post-stroke, data not shown). We further determined genotype differences in the expressions of $\alpha 2\delta$ -1 and PSD-95 at 6 months. In age-matched sham mice, we did not observe a genotype difference. In the stroked animals, $\alpha 2\delta$ -1 expression in the BDNF^{M/M} mice was significantly elevated only in the contralateral hemisphere while PSD-95 mRNA levels were not differed among sham, post-stroke WT or BDNF^{M/M} brains (Figure 2C and D). Furthermore, $\alpha 2\delta$ -1 protein expression was also increased only in the contralateral hemisphere at this time (Figure 2E and F), paralleling the $\alpha 2\delta$ -1 gene upregulation. The selective increase in the expression of $\alpha 2\delta$ -1 along with elevated TSP2 expression in the contralateral hemisphere

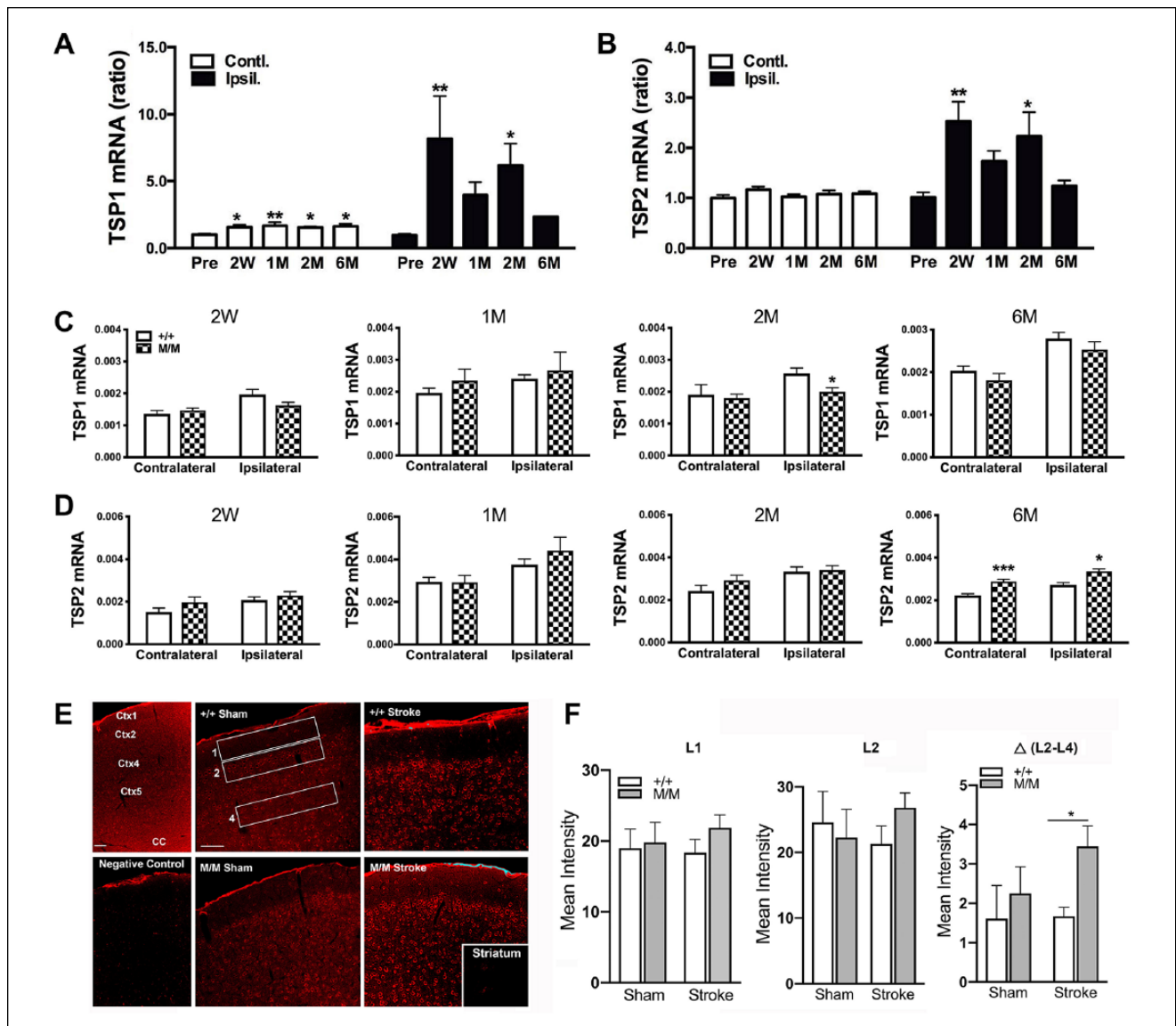


Figure 1. TSP1 and TSP2 genes (TSP, thrombospondin) expressions in $BDNF^{+/+}$ (wild type, WT) and $BDNF^{M/M}$ (BDNF, brain-derived neurotrophic factor) mice. Panels A and B: Temporal gene profiles of TSP1 (A) and TSP2 (B) in the brain following middle cerebral artery occlusion (MCAO) in WT mice. mRNA levels were measured in tissue (+2.8 to -3.8mm from bregma that covered an infarct region) from the contralateral and ipsilateral hemisphere in $BDNF^{+/+}$ mice prior to stroke (Pre) and during stroke recovery phase (2 weeks to 6 months) and normalized by actin. Y-axis represents ratios of TSP1 and TSP2 mRNA levels compared with baseline (pre) value. $N = 4-5/\text{group}$, one-way analysis of variance, Post hoc comparison. * $P < .05$, ** $P < .01$ versus Pre. W, weeks; M, months. Panels C and D: TSP1 and TSP2 genes expressions in $BDNF^{+/+}$ and $BDNF^{M/M}$ mice during the stroke recovery period. mRNA levels of TSP1 (C) and TSP2 (D) at 2 weeks (W), 1, 2, and 6 months (M) after stroke. $N = 6-7/\text{genotype}$, Student's t test * $P < .05$, *** $P < .001$, $+/+$ (WT) vs M/M , $BDNF^{M/M}$. E: Confocal microscopic assessment of TSP immunoreactivity in the cerebral cortex of WT and $BDNF^{M/M}$ mice 6 months after stroke. Representative micrographs containing cerebral cortex layers 1, 2/3, and 4 of a contralateral hemisphere of age-matched WT and $BDNF^{M/M}$ sham and stroke mice. Identical immunolabeling procedure without the primary antibody served as a negative control (not shown). Two images of the cerebral cortex that included layers 1 to 4 were captured at $20\times$ (water objective) for each animal while their identities were blinded. A composite of all the pictures was created and adjusted in Photoshop simultaneously. Scale bar = 100 μm . F: Mean optical densities of the defined rectangular areas in the cortex were assessed using Image J. Mean intensity of L1 and L2 was determined for each group, then the difference between the mean densities of L2 and L4 was calculated. Mean optical intensity in cerebral cortex was expressed as mean \pm SEM (standard error of the mean) for TSP immunoreactivity. Ctx, cortex; CC, corpus callosum. Statistical analysis was performed using 2-way analysis of variance for the effect of genotype and stroke and post hoc Fisher's LSD (least significant difference) test. $N = 5$ animals for M/M -sham and $+/+$ -sham ($N = 5$ each), M/M -stroke ($N = 6$) and $+/+$ -stroke ($N = 7$). From each animal, one randomly picked section underwent the immunohistochemical procedure.

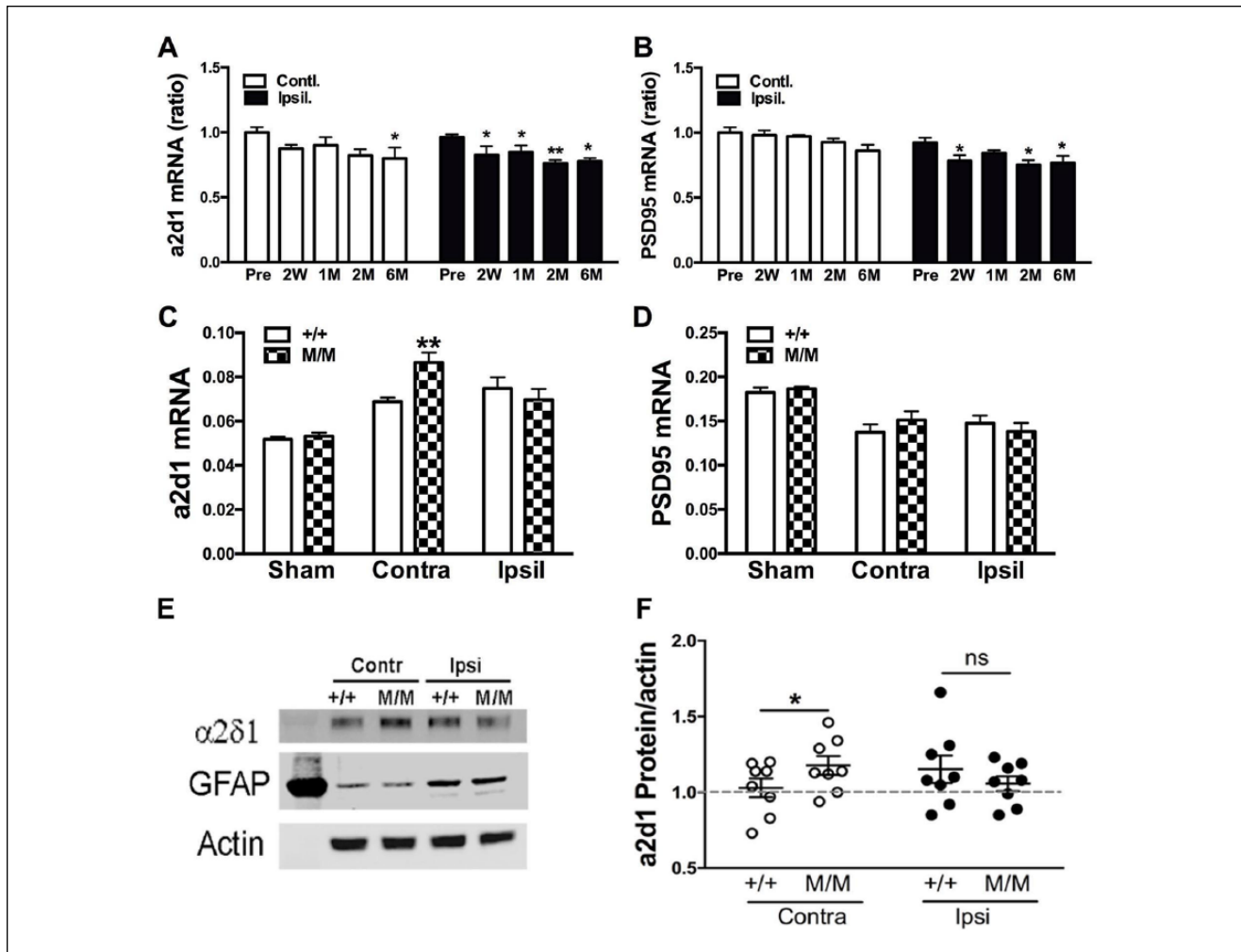


Figure 2. Expressions of $\alpha 2\delta$ -1 and PSD-95 in sham and post-stroke WT and BDNF^{M/M} (WT, wild type; BDNF, brain-derived neurotrophic factor) mice. Panels A and B: Temporal genes expressions of $\alpha 2\delta$ -1 (A) and PSD-95 (PSD, postsynaptic density) (B) in the brain following middle cerebral artery occlusion (MCAO). mRNA levels in the contralateral and ipsilateral hemisphere were measured prior to stroke (Pre) and during stroke recovery phase (2 weeks to 6 months) and normalized by actin. Y-axis represents ratios of $\alpha 2\delta$ -1 and PSD-95 mRNA levels compared with baseline pre value. N = 4-5/time point, Student's t test * $P < .05$, ** $P < .01$ versus Pre. Panels C and D: $\alpha 2\delta$ -1 (C) and PSD-95 (D) mRNA levels in age-matched sham, and stroked WT and BDNF^{M/M} mice 6 months post-stroke. N = 6-7/genotype, Student's t test * $P < .05$, ** $P < .01$ versus +/+ (WT), M/M, BDNF^{M/M} mice. Panels E and F: Expression of $\alpha 2\delta$ -1 protein in the brain of WT and BDNF^{M/M} mice at 6 months after stroke. Expression was normalized to actin and expressed as ratios to sham (interblot control, indicated by dotted line). To normalize interblot variability, an identical set of samples was loaded in each blot as an internal control and the density of the internal standard sample was used to standardize samples in multiple blots. Wilcoxon, nonparametric test was used for comparison between WT (+/+) and BDNF^{M/M} (M/M) mice. N = 8/genotype, contra, contralateral; ipsi, ipsilateral.

suggests a potential shift of synaptic balance toward excitation in this nonstroked hemisphere of BDNF^{M/M} mice.

Selective Increase in $\alpha 2\delta$ -1 Immunoreactivity in the Contralateral Cortical Layers 1/2 of BDNF^{M/M} Mice

The selectively increased expression of TSP2/ $\alpha 2\delta$ -1 in the contralateral hemisphere led us to determine the subregion specificity. Localization of $\alpha 2\delta$ -1 protein was assessed in

the dorsolateral striatum, medial striatum, layer 5 of somatosensory cortex and layer 1 of somatosensory cortex in the contralateral hemisphere (Figure 3A). Optical density measurements revealed a significant ($P = .031$, Kruskal-Wallis mean rank difference = 8.943) and robust (101%) increase of $\alpha 2\delta$ -1 immunoreactivity in layer 1 of cortex of BDNF^{M/M} stroke mice compared to that of BDNF^{M/M} sham (Figure 3B). No difference was found in brain areas of WT mice. Layer 5 of cortex also exhibited an increase in the stroked BDNF^{M/M} brains, relative to sham-treated BDNF^{M/M} (74%)

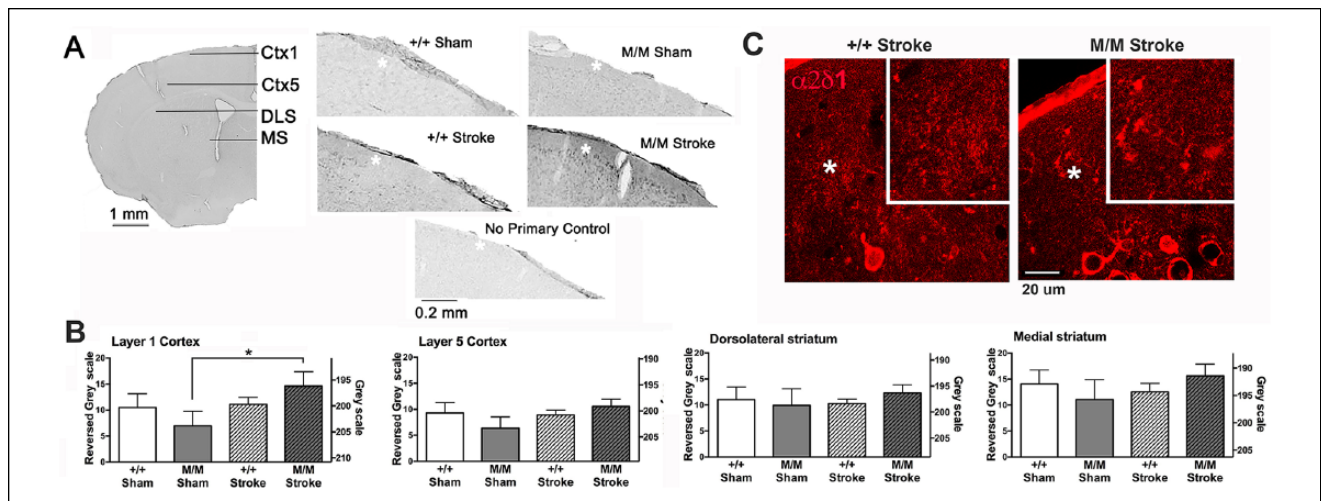


Figure 3. Light microscopic assessment of $\alpha 2\delta$ -1 immunoreactivity in the different brain regions of contralateral hemisphere in WT and $BDNF^{M/M}$ (WT, wild type; BDNF, brain-derived neurotrophic factor) sham and 6 months post-stroke mice. Panel A: Representative micrographs of a hemisections containing cerebral cortex layers I (Ctx1) and 5 (Ctx5), and the dorsolateral and medial striatum (DLS, MS) of a contralateral hemisphere of age-matched WT and $BDNF^{M/M}$ sham and stroke mice immunolabeled for $\alpha 2\delta$ -1 using silver-intensified gold (SIG) as the immunolabel. Portions of Ctx1 (white asterisks) of representative sections from the 4 groups are also shown. A portion of a section of an M/M sham animal that underwent an identical immunolabeling procedure but with the primary antibody omitted is shown at the bottom. A $100\times$ (oil objective) immunofluorescent image of $\alpha 2\delta$ -1 in a $BDNF^{M/M}$ (M/M) stroke animal was captured using an inverted Nikon Eclipse Ti-U confocal microscope. The region shown is cortical layers I and 2, with cell bodies in layer 2. Panels in B show mean \pm SEM (standard error of the mean) values of optical density measurements reflecting $\alpha 2\delta$ -1 immunoreactivity from each group, based on images detected using SIG as the label. Optical densities of dorsal striatum, medial striatum, layer 1 and layer 5 of overlying cerebral cortex were assessed using Image J's rectangle selection of area to analyze the mean gray value under the tool, Histogram. Statistical analysis was performed for 4 brain regions separately. Gray scale values (right Y-axis) obtained from each brain region were assessed for each brain. The difference in the measured greyscale values from the background values obtained from primary antibody omitted sections was plotted using reversed gray scale (left Y-axis), whereby the background was set to equal zero. Multiple comparisons revealed a significant effect of $BDNF^{M/M}$ stroke brains in layer 1 of cerebral cortex, relative to $BDNF^{M/M}$ sham brains. No other region showed significant changes evoked by stroke or genotype. $N = 5$ animals for M/M sham and +/+ sham, $N = 7$ animals for M/M stroke and +/+ stroke. From each animal, one randomly picked section underwent the immunocytochemical procedure.

but this increase did not reach statistical significance ($P = .07$ Kruskal-Wallis mean rank difference = 7.343). Neither the dorsolateral nor the medial sectors of dorsal striatum revealed any genotype or treatment effect. Higher magnification confocal micrographs showed visible $\alpha 2\delta$ -1 immunofluorescence in layer 1 of cerebral cortex, with strong staining visible in cell bodies of layer 2 (Figure 3C).

Increased Axospinous Excitatory Synapses in the Contralateral Cortex and Dorsal Striatum of $BDNF^{M/M}$ Mice

The increased $\alpha 2\delta$ -1 immunoreactivity in layers 1/2 of the cortex in $BDNF^{M/M}$ stroke mice led us to investigate potential increases of excitatory synapses in the contralateral hemisphere of $BDNF$ SNP mice. EM quantification of the areal density of excitatory axo-spinous synapses in layer 1 revealed a small but nearly significantly greater spine density for the $BDNF^{M/M}$ tissue than of WTs that was

recovering from stroke (8% increase, $P = .055$) (Figure 4C). Similarly, EM analysis of the areal frequency of axo-spinous excitatory synapses in dorsal striatum revealed a significantly higher spine density in $BDNF^{M/M}$ tissue than of WTs that were recovering from stroke (10% increase, $P = .018$) (Figure 4D). No genotype difference in the areal density of axo-spinous excitatory synapses was detected among the sham-treated animals.

Reduced GABAergic Innervation of Spiny Dendrites in Layer I and Cell Bodies of Layer 5 Pyramidal Neurons in Cortex of $BDNF^{M/M}$ Animals

Excitability of neurons is determined by the balance between inhibition and excitation. To investigate the possibility of enhanced excitability of cerebral cortical neurons due to reduced GABAergic inputs, GABAergic innervation of pyramidal cell bodies in layer 5 of cortex was assessed (Figure 5A-E). $BDNF^{M/M}$ animals showed significant

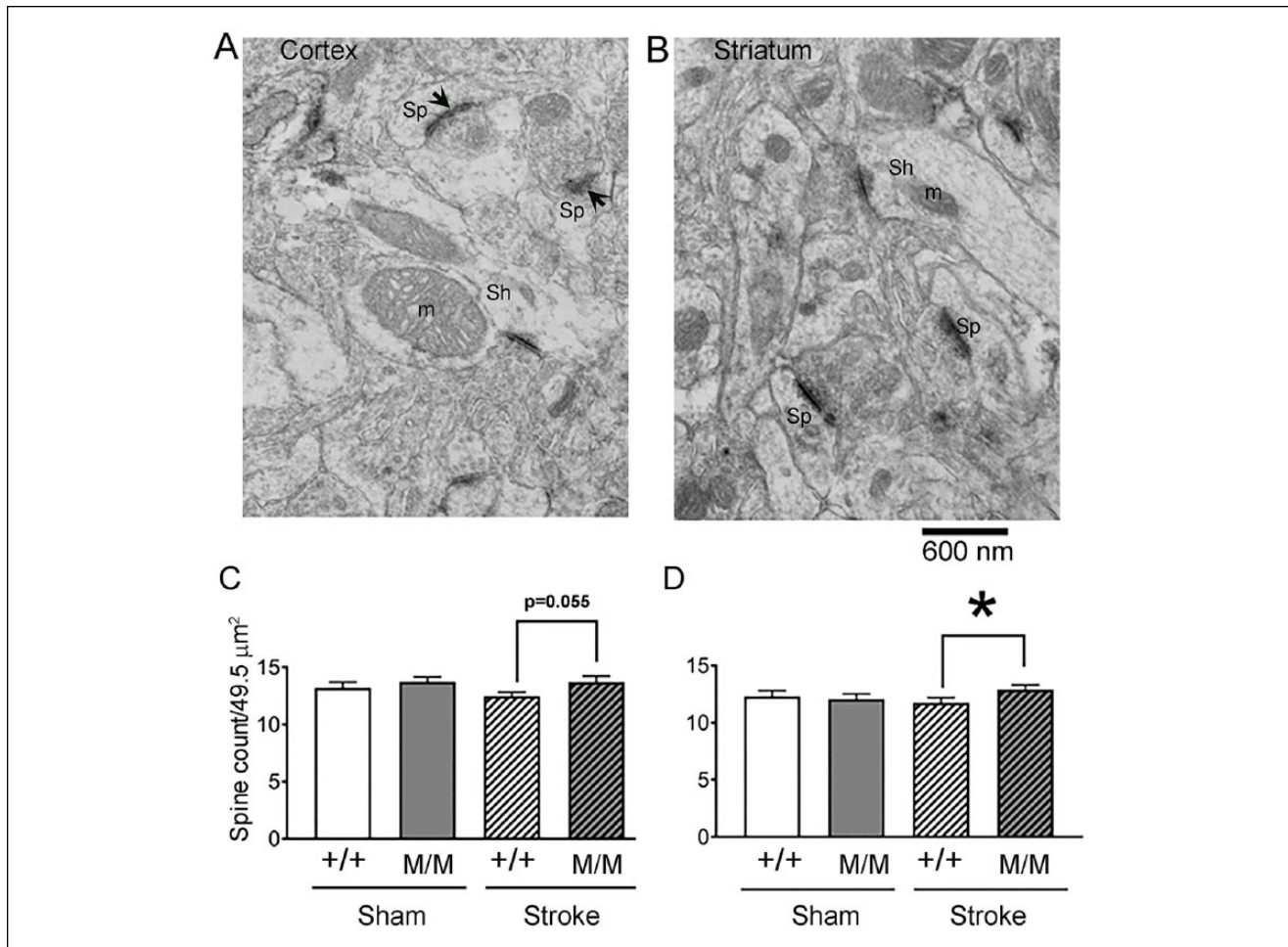


Figure 4. Spine counts per unit area in layer I of cortex and striatum. A and B: Representative electron micrographs taken from layer I of the cerebral cortex of WT (+/+) and BDNF^{M/M} (M/M) sham or 6 months post-stroke animals. Excitatory synapses formed on spines (Sp) were identified based on thick postsynaptic densities (PSDs, arrows), and absence of mitochondria (m) and presence of presynaptic vesicles. The number of axo-spinous synapses per micrograph was counted. Excitatory synapses formed on shafts (Sh) were distinguished from axo-spinous synapses, based on the presence of mitochondria and were excluded from the quantification. C and D: Quantification of the average number of spines encountered per micrograph in the layer I of cerebral cortex (C) and the dorsolateral striatum (D). Areal densities of excitatory axo-spinous synapses, were analyzed in 5 micrographs per brain, each captured at a magnification of 20000 \times , spanning a synaptic neuropil equal to 49.5 μm^2 . The bars represent the mean \pm SEM (standard error of the mean) values of the 4 groups consisting of the genotype +/+, M/M and the treatments of sham versus stroke. $P = .055$ (+/+ stroke vs M/M stroke); asterisk represents $P < .05$. For both regions, $N = 50$ for each sham group (10 micrographs/animal \times 5 animals) and $N = 70$ (10 micrographs/animal \times 7 animals) for each stroke group.

reduction of GABAergic innervation at pyramidal cell bodies following sham, compared with WT sham ($P = .0208$) and similarly to stroked WT or BDNF^{M/M} brains, indicating that the reduced GABAergic innervation is an intrinsic property associated BDNF^{M/M} phenotype.

The extent of GABAergic axon terminals forming inhibitory synapses onto dendrites of pyramidal cells was measured by using spines protruding from dendritic shafts to identify pyramidal cell dendrites (Figure 5F-H). There was a significant 45% reduction of the percent of the plasma membrane of spiny dendrites' shafts contacted by

GAD⁺ axon terminals in layer 1 of BDNF^{M/M} sham mice, relative to WT sham mice (Figure 5H). For the stroke-treated animals, there was also a significant decrease by 47% in the extent of synapses formed by GAD⁺ axon terminals along dendritic plasma membranes of pyramidal neurons of BDNF^{M/M} tissue, compared with WT tissue. Altogether, the increase of excitatory synapses, combined with the decrease of inhibitory synapses specifically in layer 1 of cortex suggests an overall greater excitability of cortical pyramidal neurons following stroke in BDNF^{M/M} brain compared with WT.

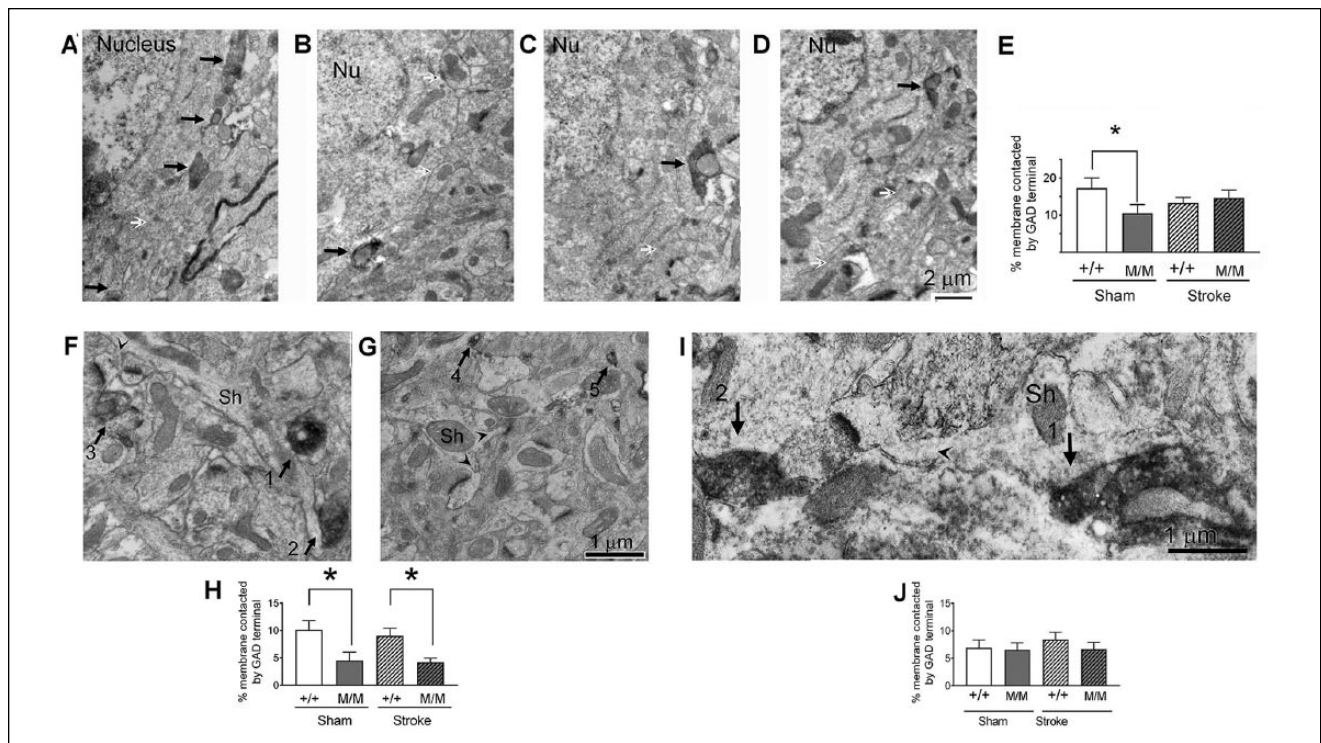


Figure 5. GABAergic (GABA, γ -aminobutyric acid) innervations of excitatory and inhibitory neurons in cortex and striatum were analyzed within brains of WT and $BDNF^{M/M}$ (WT, wild type; BDNF, brain-derived neurotrophic factor) sham and 6 months post-stroke mice. Three brain regions were analyzed: Layer 1 of cerebral cortex (for the analysis of inhibitory synapses onto spiny dendrites of pyramidal neurons), layer 5 of cerebral cortex (for the analysis of inhibitory synapses onto layer 5 pyramidal neurons' cell bodies), and dorsolateral striatum for the analysis of inhibitory synapses onto medium spiny neurons (MSN). Panels A through D show representative GABAergic innervations of pyramidal cell bodies in layer 5 of cerebral cortex in age-matched WT and $BDNF^{M/M}$ sham and 6 months stroke mice. WT (+/+) sham (A), $BDNF^{M/M}$ (M/M) sham (B), WT stroke (C) and $BDNF^{M/M}$ stroke (D). Black arrows point to the plasma membrane that is postsynaptic to GABAergic terminals, indicated by the HRP-DAB reaction product reflecting immunoreactivity to GAD. Nu = nucleus. White arrows point to portions of the plasma membrane that are not receiving GABAergic synaptic input. Micrographs were taken at a magnification of 10000 \times . E: Quantification of the percent of the plasma membrane of cell bodies contacted by GAD terminals in this region. Here and in other graph panels, asterisk indicates significance at $*P < .05$. The bars represent the mean \pm SEM (standard error of the mean) values of the 4 groups consisting of the genotype WT (+/+) or $BDNF^{M/M}$ (M/M) and the treatments of sham versus stroke. N = 19 for WT sham (4 to 5 cell bodies per animal \times 4 animals), 18 for M/M sham (4 to 5 cells per animal \times 4 animals), 30 for WT stroke (4 to 5 cells per animal \times 7 animals), and 31 for M/M stroke (4 to 5 cells per animal \times 7 animals). Panels F and G show GABAergic innervation of spiny dendrites in layer 1 of cerebral cortex from WT (+/+, F) and $BDNF^{M/M}$ (M/M, G) 6 months post-stroke animals. Arrowheads indicate the points where spine heads connect to parent dendritic shafts (Sh). Arrows point to GABAergic axon terminals in the field, indicated by the HRP-DAB (horseradish peroxidase-3,3'-diaminobenzidine) reaction product reflecting immunoreactivity to GAD. Arrows 1 and 2 show direct contact between GABAergic terminals and spiny dendrites, while arrows 3, 4, and 5 show GABAergic terminals in the plane of section but without contact with the spiny dendrites. All micrographs were captured at a magnification of 20000 \times , spanning an area equaled to 49.5 μm^2 . H: Quantification of the percent of the plasma membrane of spiny dendrites contacted by GABAergic terminals in this region. N = 50 for +/+ sham (10 dendrites per animal \times 5 animals), 50 for M/M sham (10 dendrites per animal \times 5 animals), 70 for +/+ stroke (10 dendrites per animal \times 7 animals), and 70 for M/M stroke (10 dendrites per animal \times 7 animals). Panel I shows a representative MSN from a WT stroke striatum receiving GABAergic innervations. The arrowhead indicates the point where the spine head connects to its parent dendritic shaft (Sh) that has been pseudo-colored light blue to enhance visibility of the MSN's irregular contour within this electron micrograph. Arrows point to GABAergic terminals in the field, indicated by the HRP-DAB reaction product reflecting immunoreactivity to GAD. Arrow 1 shows direct contact between a GABAergic terminal and the MSN while arrow 2 shows a GABAergic terminal in the plane of the section but without visible contact with the MSN. The electron micrograph was taken at a magnification of 30000 \times . Panel J shows quantification of the percent of the plasma membrane of MSNs contacted by GABAergic terminals in striatum. N = 50 for +/+ sham (10 dendrites per animal \times 5 animals), 50 for M/M sham (10 dendrites per animal \times 5 animals), 70 for +/+ stroke (10 dendrites per animal \times 7 animals), and 70 for M/M stroke (10 dendrites per animal \times 7 animals). For the assessment of the proportion of layer 5 pyramidal cell body plasma membrane contacted GABAergic axosomatic synapse lengths, 5 cell bodies per brain region per animal were analyzed. To assess the proportion of the plasma membrane of spiny dendrites in layer 1 and dorsal striatum that were contacted by GABAergic axon terminals, 10 dendritic profiles were sampled from each brain, using electron micrographs that were captured at a magnification of 25000 \times .

GABAergic Innervation of MSN in Striatum Is Not Affected by the Genotype or Treatment

BDNF is synthesized by cortical neurons projecting to striatum but is not known to be synthesized by neurons in the striatum. As expected, the genotype BDNF^{M/M} showed no effect on GABAergic innervation of MSNs in striatum, all of which arise from local inhibitory neurons or axon collaterals of MSNs located within striatum. Moreover, although the occurrence of excitatory synapses on MSNs was increased by the treatment of stroke of BDNF^{M/M} animals, this treatment had no effect on the extent of GABAergic innervation of MSNs (Figure 5I and J). The increase of excitatory synapses without a change in inhibitory synapses would result in enhanced overall excitability of MSNs of BDNF^{M/M} brains.

Discussion

Stroke induces changes in molecular expression, structural plasticity, and behavioral adaptation at acute, subacute, and long-term recovery phases. The temporal and spatial changes through multiple stages in chronic stroke suggest that a single molecule may exert differential effect(s) during specific stages of recovery, presumably through interaction with different molecules. Our previous study addressed the impact of the genetic variant of *bdnf*, val66met on stroke. The results showed that mice homozygous for the val66met allele (BDNF^{M/M}) display a biphasic response: greater behavior impairment during the acute phase but better function during recovery phases compared to WT mice.¹⁰ The observed spontaneous motor recovery starting at 2 weeks could be due to reestablishment of the excitatory/inhibitory balance within the direct pathways. On the other hand, reverberating excitatory input through the cortico-striatal-thalamic circuit depicted in Figure 6 may account for superior behavioral adaptation of BDNF^{M/M} mice in the later, chronic phase. Prominent motor/gait improvement in ipsilesional limb during recovery was associated with elevated expression of vesicular glutamate transporters VGLUT1 and 2 and excitatory synaptic molecules in the contralateral striatum.¹⁰ One aim of the current study was to assess whether the superior behavioral adaptation of BDNF^{M/M} mice occurs through the expression of molecules that can boost the function of the excitatory cortico-striatal synaptic pathway within the less affected contralateral hemisphere. The significantly increased expressions of TSP1/2 were shown at 2 weeks and 2 months, but not at 1 month during recovery phase in WT stroke mice. The biphasic profile in the molecular expression within a complete context of stroke stages suggests that the acute neurotoxic and inflammatory milieu induced by stroke is replaced by a more permissive environment that facilitates the repair/recovery processes. Indeed, we demonstrated that BDNF^{M/M} mice express higher TSP2 mRNA and

TSP proteins in layer 2 of the contralateral cerebral cortex at 6 months of recovery from stroke, which is consistent with the greater ensheathment of synaptic clefts by astrocytes in layers 2/3.³⁴ This coincides with the increased expression of mRNA for its neuronal receptor $\alpha 2\delta$ -1, known to be an excitatory synaptogenesis agent. Moreover, LM- and EM-immunocytochemistry, together, revealed that the protein level is elevated detectably in layers 1/2 of cerebral cortex, which further demonstrates a sustained involvement of TSPs / $\alpha 2\delta$ -1 in a region-specific manner.

A second aim of the current study was to characterize the ultrastructural and synaptic bases for the enhanced compensatory motor function in these BDNF^{M/M} mice following chronic stroke. Neuronal activity regulates BDNF secretion, which is important for synaptic plasticity.³⁷⁻⁴⁰ The balance between excitation and inhibition at the level of synapses is critical in processing sensory information, synaptogenesis, motor activity, and cognitive function.^{23,41-43} Imbalance between excitation and inhibition is implicated in neurological disorders⁴⁴⁻⁴⁶ and may be manifested immediately following stroke and during the recovery phase from stroke. In this study, the use of BDNF^{M/M} that exhibits selective impairment of activity-dependent, but not constitutive BDNF bioavailability allowed us to address the role of activity-dependent BDNF release in synaptic plasticity during the delayed recovery phase following stroke. Previous studies showed that activity-dependent *bdnf* transcription promotes inhibitory synapse maturation and sets the network-level adaptation for synaptic balance.⁴⁷⁻⁴⁹ Thus, BDNF^{M/M} mice with reduced stroke-induced BDNF secretion may have led to the reduction of inhibitory synapses that we detected, yielding a shift toward increased excitatory-to-inhibitory synapse balance onto pyramidal cells in cortex as late as 6 months post-stroke.

Although biochemical and LM analyses of brain regions preclude assessments at the cellular and synaptic levels, our rigorous EM data align well with the biochemical and LM data: indeed, we demonstrated that excitatory synapses onto excitatory pyramidal cells were greater in layer 1 of the cerebral cortex of BDNF^{M/M} mice that underwent stroke, compared with the level seen for WT littermates. This supports the idea that the augmented level of TSP2/ $\alpha 2\delta$ -1 within cortex promoted synaptogenesis following stroke, especially by excitatory pyramidal cells of BDNF^{M/M} cortex. We propose that the overall excitation of the cortico-striatal pathway may underlie enhanced functional recovery in chronic stroke of BDNF^{M/M} mice. The findings indicate that layers 1/2 of cortex is one main site of synaptic plasticity exhibiting shifts in synaptic balance toward greater excitation in the contralateral striatum of BDNF^{M/M} mice at 6 months post-stroke.

A number of studies have shown that somatosensory cortex,^{50,51} the cerebral cortical region that we analyzed, participates in motor learning in this study. It was demonstrated

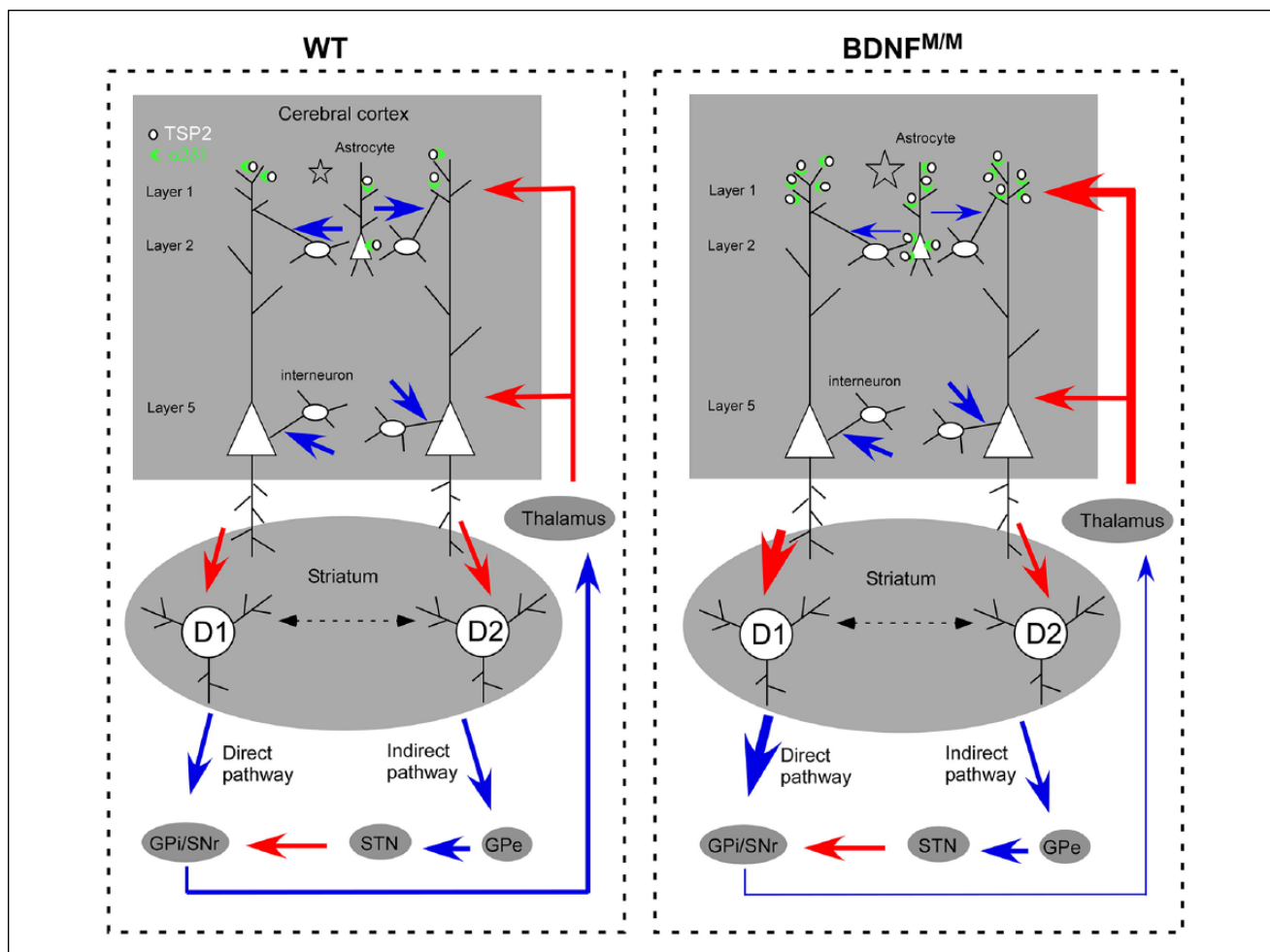


Figure 6. A proposed schematic diagram for the involvement of cortico-striatal pathway for behavioral adaptation during stroke recovery. The contralateral cortico-striatal drive favors a direct pathway in $BDNF^{M/M}$ which contributes to the improved motor function during long-term recovery. The thickness of lines indicates the strength of the connection (red arrow, excitatory glutamatergic; blue arrow, inhibitory GABAergic). Compared with WT mice following stroke, $BDNF^{M/M}$ mice exhibited synaptic changes reflecting decreased inhibition from interneurons (disinhibition, thereby excitation), together with augmented excitatory synaptogenesis in layers 1/2, supported by increased TSP2 expression from astrocytes and increased levels of TSP2 receptor $\alpha 2\delta-1$ in layers 1/2 of cerebral cortex. In dorsal striatum, inputs from layer 5 pyramidal neurons form synapses with medium spiny neurons expressing dopamine D1 and D2 receptors, which partakes in the direct and indirect pathways, respectively. Enhanced excitatory input to dorsal striatum favoring the direct pathway which then inhibits inhibitory input to thalamus (disinhibition) could result in reverberating excitation of the circuit comprised of the cortico-basal ganglia-thalamo-cortical loop and promotes motor/gait function in $BDNF^{M/M}$ mice. The ventromedial thalamus relays input from substantia nigra pars reticulata³⁵ to cortex, specifically targeting layer 1.³⁶ The combined data demonstrated that the layers 1/2 of cortex as the major subregion for synaptic plasticity.

that the somatosensory cortex of mice plays an important role in forelimb motor adaptation, such as updating motor commands as needed in order to reduce error of an acquired motor skill involving pulling of a joystick.⁵² It is likely that the challenge of regaining gait following stroke demands update of motor commands involving synaptic plasticity of the somatosensory cortex that is then propagated to plasticity of the cortico-striatal pathway. In support of this idea, we showed that cell bodies of layer 5 pyramidal neurons, which are the population of pyramidal neurons in

somatosensory cortex that project to striatum, receive less GABAergic innervation, indicating increased excitability of these cells and increased cortico-striatal drive.

The striatum is a major subcortical structure for activity-dependent synaptic plasticity⁵³ and also important for motor learning related to rotarod performance, as the mice lacking the excitatory receptor subunit NMDAR1 in the striatum exhibit disrupted motor learning and synaptic plasticity in the striatum.⁵⁴ Therefore, we predicted that striatum would be the subregion that upregulates excitatory

markers in the contralateral hemisphere of BDNF^{M/M} mice. However, synaptic plasticity is a basis for alteration of neuronal circuitry and functions, not restricted to discrete brain regions, such as the striatum. The excitatory afferents from cortex and thalamus project to striatal interneurons and MSNs.⁵⁵ These striatal neurons form the direct and indirect connections.⁵³ The direct pathway provides information on movement planning, initiation and motor sequence selection, which facilitates movements. The indirect pathway suppresses movements that would conflict with ongoing selected movements.⁵⁶ The enhanced motor/gait function in BDNF^{M/M} mice post-stroke suggests that the direct pathway may be more involved (Figure 6). The enhanced output of inhibitory MSNs in the striatum may exert excitatory motor signal through ventromedial thalamus,^{35,36} thereby intensifying excitation through the cortico-striatal-thalamic pathway. This view is consistent with the known role of inhibitory basal ganglia circuit for inducing excitatory signal from thalamus to cortex.⁵⁷ In particular, since the ventromedial thalamic input to cortex is predominant in layer 1,^{36,58} the increase specifically in layer 1 of both excitatory synaptogenesis and $\alpha 2\delta$ -1-immunoreactivity provides further support for the view that the direct pathway from basal ganglia is more involved than the indirect pathway. Future electrophysiology studies will address whether the cellular and molecular changes that we detected indeed reflect enhanced synaptic activity in the direct pathway.

In summary, increased expression of excitatory synaptic markers TSP2 and $\alpha 2\delta$ -1 in the BDNF^{M/M} mice is associated with superior functional recovery from stroke. Systematic analyses of excitatory and inhibitory synapses in subregions of contralateral hemisphere revealed that stroke increased $\alpha 2\delta$ -1 immunoreactivity, more excitatory synapses and less inhibitory synapses in layers 1/2 of cortex, indicating layers 1/2 of contralateral cortex to be a main site for synaptic plasticity. In the striatum, there is an increase in excitatory synapses with no changes in the inhibitory synapses, yielding a synaptic circuit that is overall more excitable. An increase in excitatory-to-inhibitory ratio in cortico-basal ganglia pathway may underlie the enhanced functional recovery of ipsilesional limbs in BDNF^{M/M} mice, suggesting the importance of neural circuit for behavior adaptation in recovery function in neurological disorders.

Acknowledgments

We thank E. Ivanova and Structural and Functional Imaging Core at the Burke Neurological Institute for the technical assistance.

Declaration of Conflicting Interests

The authors declared no potential conflicts of interest with respect to the research, authorship, and/or publication of this article.

Funding

The authors disclosed receipt of the following financial support for the research, authorship, and/or publication of this article: Funding sources: National Institute of Health awards, NINDS R01NS077897 (SC), R01NS095359-10 (SC), and the Burke Foundation (SC), R01 DA038616 (CA), R21MH105846 (CA), P30 EY13079 (CA).

ORCID iD

Hannah S. Actor-Engel  <https://orcid.org/0000-0002-4602-680X>

References

1. Minichiello L. TrkB signalling pathways in LTP and learning. *Nat Rev Neurosci.* 2009;10:850-860.
2. Bekinschtein P, Cammarota M, Izquierdo I, Medina JH. BDNF and memory formation and storage. *Neuroscientist.* 2008;14:147-156.
3. Chen ZY, Jing D, Bath KG, et al. Genetic variant BDNF (Val66Met) polymorphism alters anxiety-related behavior. *Science.* 2006;314:140-143.
4. Balkaya M, Cho S. Genetics of stroke recovery: BDNF val66met polymorphism in stroke recovery and its interaction with aging. *Neurobiol Dis.* 2019;126:36-46.
5. Siironen J, Juvela S, Kanarek K, Vilkkii J, Hernesniemi J, Lappalainen J. The Met allele of the BDNF Val66Met polymorphism predicts poor outcome among survivors of aneurysmal subarachnoid hemorrhage. *Stroke.* 2007;38:2858-2860.
6. Kim JM, Stewart R, Park MS, et al. Associations of BDNF genotype and promoter methylation with acute and long-term stroke outcomes in an East Asian cohort. *PLoS One.* 2012;7:e51280.
7. Cramer SC, Procaccio V; GAIN Americas; GAIN International Study Investigators. Correlation between genetic polymorphisms and stroke recovery: analysis of the GAIN Americas and GAIN International Studies. *Eur J Neurol.* 2012;19:718-724.
8. Mirowska-Guzel D, Gromadzka G, Czlonkowski A, Czlonkowska A. BDNF -270 C>T polymorphisms might be associated with stroke type and BDNF -196 G>A corresponds to early neurological deficit in hemorrhagic stroke. *J Neuroimmunol.* 2012;249:71-75.
9. Mirowska-Guzel D, Gromadzka G, Mendel T, et al. Impact of BDNF -196 G>A and BDNF -270 C>T polymorphisms on stroke rehabilitation outcome: sex and age differences. *Top Stroke Rehabil.* 2014;21(suppl 1):S33-S41.
10. Qin L, Jing D, Parauda S, et al. An adaptive role for BDNF Val66Met polymorphism in motor recovery in chronic stroke. *J Neurosci.* 2014;34:2493-2502.
11. Bornstein P, Armstrong LC, Hankenson KD, Kyriakides TR, Yang Z. Thrombospondin 2, a matricellular protein with diverse functions. *Matrix Biol.* 2000;19:557-568.
12. Ullian EM, Sapperstein SK, Christopherson KS, Barres BA. Control of synapse number by glia. *Science.* 2001;291:657-661.
13. Christopherson KS, Ullian EM, Stokes CC, et al. Thrombospondins are astrocyte-secreted proteins that promote CNS synaptogenesis. *Cell.* 2005;120:421-433.

14. Risher WC, Eroglu C. Thrombospondins as key regulators of synaptogenesis in the central nervous system. *Matrix Biol.* 2012;31:170-177.
15. Eroglu C, Allen NJ, Susman MW, et al. Gabapentin receptor $\alpha 2\delta$ -1 is a neuronal thrombospondin receptor responsible for excitatory CNS synaptogenesis. *Cell.* 2009;139:380-392.
16. Risher WC, Kim N, Koh S, et al. Thrombospondin receptor $\alpha 2\delta$ -1 promotes synaptogenesis and spinogenesis via post-synaptic Rac1. *J Cell Biol.* 2018;217:3747-3765.
17. Faria LC, Gu F, Parada I, Barres B, Luo ZD, Prince DA. Epileptiform activity and behavioral arrests in mice overexpressing the calcium channel subunit $\alpha 2\delta$ -1. *Neurobiol Dis.* 2017;102:70-80.
18. Li S, Overman JJ, Katsman D, et al. An age-related sprouting transcriptome provides molecular control of axonal sprouting after stroke. *Nat Neurosci.* 2010;13:1496-1504.
19. Nudo RJ. Functional and structural plasticity in motor cortex: implications for stroke recovery. *Phys Med Rehabil Clin N Am.* 2003;14(1 suppl):S57-S76.
20. Clarkson AN, Huang BS, Macisaac SE, Mody I, Carmichael ST. Reducing excessive GABA-mediated tonic inhibition promotes functional recovery after stroke. *Nature.* 2010;468:305-309.
21. Lin TN, Kim GM, Chen JJ, Cheung WM, He YY, Hsu CY. Differential regulation of thrombospondin-1 and thrombospondin-2 after focal cerebral ischemia/reperfusion. *Stroke.* 2003;34:177-186.
22. Zhou HJ, Zhang HN, Tang T, et al. Alteration of thrombospondin-1 and -2 in rat brains following experimental intracerebral hemorrhage. Laboratory investigation. *J Neurosurg.* 2010;113:820-825.
23. Brown P, Ridding MC, Werhahn KJ, Rothwell JC, Marsden CD. Abnormalities of the balance between inhibition and excitation in the motor cortex of patients with cortical myoclonus. *Brain.* 1996;119(pt 1):309-317.
24. Qin L, Kim E, Ratan R, Lee FS, Cho S. Genetic variant of BDNF (Val66Met) polymorphism attenuates stroke-induced angiogenic responses by enhancing anti-angiogenic mediator CD36 expression. *J Neurosci.* 2011;31:775-783.
25. Cho S, Park EM, Febbraio M, et al. The class B scavenger receptor CD36 mediates free radical production and tissue injury in cerebral ischemia. *J Neurosci.* 2005;25:2504-2512.
26. Kim E, Tolhurst AT, Cho S. Dereglulation of inflammatory response in the diabetic condition is associated with increased ischemic brain injury. *J Neuroinflammation.* 2014;11:83.
27. Kim E, Febbraio M, Bao Y, Tolhurst AT, Epstein JM, Cho S. CD36 in the periphery and brain synergizes in stroke injury in hyperlipidemia. *Ann Neurol.* 2012;71:753-764.
28. Kim E, Woo MS, Qin L, et al. Daidzein augments cholesterol homeostasis via ApoE to promote functional recovery in chronic stroke. *J Neurosci.* 2015;35:15113-15126.
29. Bauer CS, Nieto-Rostro M, Rahman W, et al. The increased trafficking of the calcium channel subunit $\alpha 2\delta$ -1 to presynaptic terminals in neuropathic pain is inhibited by the $\alpha 2\delta$ -1 ligand pregabalin. *J Neurosci.* 2009;29:4076-4088.
30. Aoki C, Chen YW, Chowdhury TG, Piper W. $\alpha 4\beta\delta$ -GABAA receptors in dorsal hippocampal CA1 of adolescent female rats traffic to the plasma membrane of dendritic spines following voluntary exercise and contribute to protection of animals from activity-based anorexia through localization at excitatory synapses. *J Neurosci Res.* 2018;96:1450-1466.
31. Chen YW, Actor-Engel H, Sherpa AD, Klingensmith L, Chowdhury TG, Aoki C. NR2A- and NR2B-NMDA receptors and drebrin within postsynaptic spines of the hippocampus correlate with hunger-evoked exercise. *Brain Struct Funct.* 2017;222:2271-2294.
32. Sarro EC, Kotak VC, Sanes DH, Aoki C. Hearing loss alters the subcellular distribution of presynaptic GAD and postsynaptic GABAA receptors in the auditory cortex. *Cereb Cortex.* 2008;18:2855-2867.
33. Chen YW, Surgent O, Rana BS, Lee F, Aoki C. Variant BDNF-Val66Met polymorphism is associated with layer-specific alterations in GABAergic innervation of pyramidal neurons, elevated anxiety and reduced vulnerability of adolescent male mice to activity-based anorexia. *Cereb Cortex.* 2017;27:3980-3993.
34. Lanjakornsiripan D, Pior BJ, Kawaguchi D, et al. Layer-specific morphological and molecular differences in neocortical astrocytes and their dependence on neuronal layers. *Nature Commun.* 2018;9:1623.
35. Kha HT, Finkelstein DI, Tomas D, Drago J, Pow DV, Horne MK. Projections from the substantia nigra pars reticulata to the motor thalamus of the rat: single axon reconstructions and immunohistochemical study. *J Comp Neurol.* 2001;440:20-30.
36. Herkenham M. The afferent and efferent connections of the ventromedial thalamic nucleus in the rat. *J Comp Neurol.* 1979;183:487-517.
37. Elmariah SB, Oh EJ, Hughes EG, Balice-Gordon RJ. Astrocytes regulate inhibitory synapse formation via Trk-mediated modulation of postsynaptic GABA^A receptors. *J Neurosci.* 2005;25:3638-3650.
38. Poo MM. Neurotrophins as synaptic modulators. *Nat Rev Neurosci.* 2001;2:24-32.
39. Kline DD, Ogier M, Kunze DL, Katz DM. Exogenous brain-derived neurotrophic factor rescues synaptic dysfunction in Mecp2-null mice. *J Neurosci.* 2010;30:5303-5310.
40. Suzuki S, Kiyosue K, Hazama S, et al. Brain-derived neurotrophic factor regulates cholesterol metabolism for synapse development. *J Neurosci.* 2007;27:6417-6427.
41. Maffei A, Nelson SB, Turrigiano GG. Selective reconfiguration of layer 4 visual cortical circuitry by visual deprivation. *Nat Neurosci.* 2004;7:1353-1359.
42. Buschges A, Manira AE. Sensory pathways and their modulation in the control of locomotion. *Curr Opin Neurobiol.* 1998;8:733-739.
43. Cline H. Synaptogenesis: a balancing act between excitation and inhibition. *Curr Biol.* 2005;15:R203-R205.
44. Möhler H. GABA^A receptors in central nervous system disease: anxiety, epilepsy, and insomnia. *J Recept Signal Transduct Res.* 2006;26:731-740.
45. Rubenstein JL, Merzenich MM. Model of autism: increased ratio of excitation/inhibition in key neural systems. *Genes Brain Behav.* 2003;2:255-267.
46. Wassef A, Baker J, Kochan LD. GABA and schizophrenia: a review of basic science and clinical studies. *J Clin Psychopharmacol.* 2003;23:601-640.

47. Hong EJ, McCord AE, Greenberg ME. A biological function for the neuronal activity-dependent component of BDNF transcription in the development of cortical inhibition. *Neuron*. 2008;60:610-624.
48. West AE. Biological functions of activity-dependent transcription revealed. *Neuron*. 2008;60:523-525.
49. Huang ZJ, Kirkwood A, Pizzorusso T, et al. BDNF regulates the maturation of inhibition and the critical period of plasticity in mouse visual cortex. *Cell*. 1999;98:739-755.
50. Pavlides C, Miyashita E, Asanuma H. Projection from the sensory to the motor cortex is important in learning motor skills in the monkey. *J Neurophysiol*. 1993;70:733-741.
51. Vidoni ED, Acerra NE, Dao E, Meehan SK, Boyd LA. Role of the primary somatosensory cortex in motor learning: an rTMS study. *Neurobiol Learn Mem*. 2010;93:532-539.
52. Mathis MW, Mathis A, Uchida N. Somatosensory cortex plays an essential role in forelimb motor adaptation in mice. *Neuron*. 2017;93:1493-1503.e6.
53. Kreitzer AC, Malenka RC. Striatal plasticity and basal ganglia circuit function. *Neuron*. 2008;60:543-554.
54. Dang MT, Yokoi F, Yin HH, Lovinger DM, Wang Y, Li Y. Disrupted motor learning and long-term synaptic plasticity in mice lacking NMDAR1 in the striatum. *Proc Natl Acad Sci U S A*. 2006;103:15254-15259.
55. Hunnicutt BJ, Jongbloets BC, Birdsong WT, Gertz KJ, Zhong H, Mao T. A comprehensive excitatory input map of the striatum reveals novel functional organization. *Elife*. 2016;5:e19103.
56. Reiner A, Hart NM, Lei W, Deng Y. Corticostriatal projection neurons—dichotomous types and dichotomous functions. *Front Neuroanat*. 2010;4:142.
57. Kim J, Kim Y, Nakajima R, et al. Inhibitory basal ganglia inputs induce excitatory motor signals in the thalamus. *Neuron*. 2017;95:1181-1196.e8.
58. Naka A, Adesnik H. Inhibitory circuits in cortical layer 5. *Front Neural Circuits*. 2016;10:35.